Analytical and Discrete Vortex Models for an Oscillating Flat Plate with Trailing Edge Flap

Jens Honoré Walther [a,1] Allan Larsen [b]

[a] *Danish Maritime Institute, Hjortekærsvej 99, DK-2800 Lyngby, Denmark. E-mail: jhw@danishmaritime.dk*

[b] *COWI A/S, Parallelvej 15, DK-2800 Lyngby, Denmark. E-mail: aln@cowi.dk*

Two-dimensional viscous incompressible flow past a flat plate with a half-chord trailing edge flap is simulated using a particle method. The main plate is forced in a harmonic pitch motion with an amplitude of 2° and an out-of-phase flap motion. The reduced velocity is $v_r = 10$ and the Reynolds number based on chord length is 10^4. The numerical results are compared with the inviscid solution due to Theodorsen.

Key words: Multiple bodies in individual motion. Flutter control. Discrete vortex method. Conservation of vorticity moments. Aerodynamic derivatives.

1 Introduction

Aerodynamic stability or flutter is often found to be a governing design parameter for cable supported bridges with very long spans. Past efforts to control flutter has involved increase of inertia and stiffness properties of the bridge structure, or by splitting the deck structure in two independent but rigidly connected girders separated by a large horizontal gap — the twin deck concept. An alternative approach to control of flutter is to introduce moveable control surfaces in connection with the deck structure.

An aerodynamic control system involving a box shaped main girder equipped with moveable leading and trailing edge flaps is currently being evaluated by COWI using the discrete vortex method. The present paper investigates the ability of the developed discrete vortex method to predict aerodynamic loads

[1] Corresponding author.

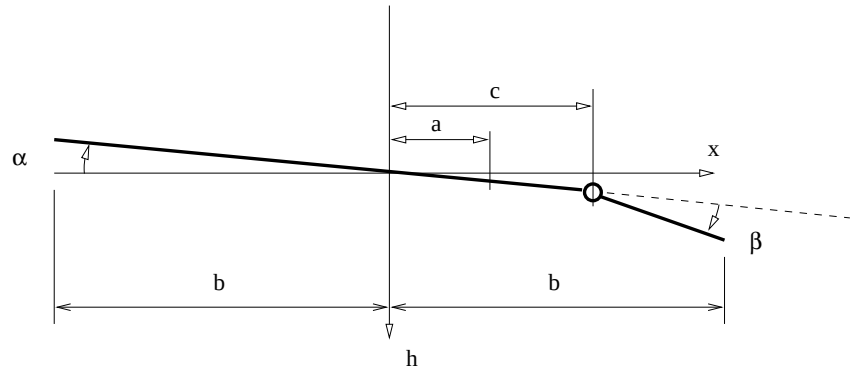

Fig. 1. Sketch of flat plate with trailing edge flap (aileron).

on a multi element structure. The investigation involves prediction of loads for the flow past a flat plate with a moveable half-chord trailing edge flap.

The results are compared with the inviscid loads on a flat plate as given by Theodorsen [1]. To secure reasonable agreement with the inviscid loads the trailing edge flap half the chord length in order to efficiently penetrate the boundary layer.

2 Governing equations

2.1 Inviscid loads on a flat plate with a training edge flap

The aerodynamic loads on a streamlined body undergoing harmonic heave and pitch motion depend on the geometry of the body, the velocity and acceleration of the body, and of the Reynolds number.

In the limit of vanishing viscosity the aerodynamic lift and moment on a flat plate with a trailing edge flap (aileron) cf. Fig. 1 is given by the well known expression by Theodorsen [1]

$$\begin{aligned} P = &-\rho b^2 \left(v\pi\dot{\alpha} + \pi\ddot{h} - \pi b a\ddot{\alpha} - vT_4\dot{\beta} - T_1 b\ddot{\beta} \right) \\ &- 2\pi\rho v b C(k) \left\{ v\alpha + \dot{h} + b\left(\frac{1}{2} - a\right)\dot{\alpha} + \frac{1}{\pi}T_{10}v\beta + b\frac{1}{2\pi}T_{11}\dot{\beta} \right\}, \end{aligned} \tag{1}$$

$$\begin{aligned} M_\alpha = &-\rho b^2 \left[\pi\left(\frac{1}{2} - a\right) vb\dot{\alpha} + \pi b^2 \left(\frac{1}{8} + a^2\right)\ddot{\alpha} + (T_4 + T_{10})v^2\beta \right. \\ &\left. + \left(T_1 - T_8 - (c-a)T_4 + \frac{1}{2}T_{11}\right) vb\dot{\beta} - \left(T_7 + (c-a)T_1\right) b^2\ddot{\beta} - a\pi b\ddot{h} \right] \end{aligned} \tag{2}$$

$$
\begin{aligned}
&+ 2\rho v b^2 \pi \left(a + \frac{1}{2}\right) C(k) \left\{ v\alpha + \dot{h} + b\left(\frac{1}{2} - a\right)\dot{\alpha} + \frac{1}{\pi} T_{10} v\beta + b\frac{1}{2\pi} T_{11}\dot{\beta} \right\}, \\
M_\beta = &-\rho b^2 \left[\pi \left(\frac{1}{2} - a\right) v b\dot{\alpha} + \pi b^2 \left(\frac{1}{8} + a^2\right)\ddot{\alpha} + (T_4 + T_{10})\, v^2\beta \right. \\
&\left. + \left(T_1 - T_8 - (c-a)T_4 + \frac{1}{2}F_{11}\right) v b\dot{\beta} - (T_1 + (c-a)T_1)\, b^2\ddot{\beta} - a\pi b\ddot{h} \right] \\
&+ 2\rho v b^2 \pi \left(a + \frac{1}{2}\right) C(k) \left\{ v\alpha + \dot{h} + b(\frac{1}{2} - a)\dot{\alpha} + \frac{1}{\pi} T_{10} v\beta + b\frac{1}{2\pi} T_{11}\dot{\beta} \right\},
\end{aligned}
\tag{3}
$$

where α is the angle of attack of the plate, and β is the angle of attack of the flap relative to the main plate. P, and M_α are the total lift and moment on the plate, and M_β is the moment on the flap. b is the half chord, a the non-dimensional centre of rotation of the plate, and c is the non-dimensional position of the flap (a and c are non-dimensionalised by b). $C(k)$ is the well known Theodorsen circulation function, and $k = b\omega/v$ the non-dimensional frequency of the motion cf. [1].

The first term in equations (1) – (3) stems from the non-circulatory flow (the surface vorticity), and the second term from the vorticity in the wake.

For completeness, the constants are listed in Appendix A.

2.2 Aerodynamic derivatives

The lift and moment on a body undergoing a harmonic pitch motion is commonly also given in terms of aerodynamic derivatives

$$
L \approx \frac{1}{2}\rho v^2 b \left(k H_2^* \frac{b\dot{\alpha}}{v} + k^2 H_3^* \alpha \right), \tag{4}
$$

$$
M \approx \frac{1}{2}\rho v^2 b^2 \left(k A_2^* \frac{b\dot{\alpha}}{v} + k^2 A_3^* \alpha \right). \tag{5}
$$

Experimentally, the H_i^* and A_i^* are extracted by performing a series of pitch tests in the valid k-range. The derivatives are here efficiently extracted using the method of Fourier averaging, thus

$$
\begin{aligned}
H_2^* &= \frac{1}{\frac{1}{2}\rho v b^2 k} \frac{\mathrm{Corr}(L, \dot{\alpha})}{\mathrm{Corr}(\dot{\alpha}, \dot{\alpha})}, \; H_3^* = \frac{1}{\frac{1}{2}\rho v^2 b k^2} \frac{\mathrm{Corr}(L, \alpha)}{\mathrm{Corr}(\alpha, \alpha)}, \\
A_2^* &= \frac{1}{\frac{1}{2}\rho v b^3 k} \frac{\mathrm{Corr}(M, \dot{\alpha})}{\mathrm{Corr}(\dot{\alpha}, \dot{\alpha})}, \; A_3^* = \frac{1}{\frac{1}{2}\rho v^2 b^2 k^2} \frac{\mathrm{Corr}(M, \alpha)}{\mathrm{Corr}(\alpha, \alpha)},
\end{aligned}
\tag{6}
$$

where $\mathrm{Corr}(x, y)$ denotes the correlation of x with y.

2.3.1 Vorticity transport equation

The governing equation for a two-dimensional laminar flow is the vorticity transport equation

$$\frac{D\omega}{Dt} = \nu \nabla \omega, \tag{7}$$

where D/Dt is the substantial derivative, and ν the kinematic viscosity. Using Euler integration, the particle approximation of (7) is

$$\vec{x}_i^{k+1} = \vec{x}_i^k + \Delta t(\vec{V}(t) + \vec{v}_i^k) + \vec{\eta}_i, \tag{8}$$

where $(\vec{x}_i^k, \Gamma_i)$ is the position and the strength of the i-th particle at the k-th time step. $\vec{v}_i$ is the "induced" velocity from the particles in the flow and $\vec{V}(t)$ is the irrotational onset flow. $\vec{\eta}_i$ are the random walks approximating diffusion cf. [2].

2.3.2 Kinematics

The kinematic relation between the velocity and the vorticity is

$$\begin{aligned}\vec{v}(\vec{x}) = &-\frac{1}{2\pi} \iint_{\mathcal{D}} \frac{\vec{\omega}_0 \times \Delta\vec{x}_0}{|\Delta\vec{x}_0|^2} \, \mathrm{d}\mathcal{D}_0 \\ &+ \frac{1}{2\pi} \oint_{\mathcal{B}} \frac{(\vec{v}_0 \cdot \vec{n}_0)\Delta\vec{x}_0 - (\vec{v}_0 \times \vec{n}_0) \times \Delta\vec{x}_0}{|\Delta\vec{x}_0|^2} \, \mathrm{d}\mathcal{B}_0,\end{aligned} \tag{9}$$

where $\Delta\vec{x}_0 = (\vec{x}_0 - \vec{x})$, $\vec{n}_0$ is the surface normal, and $\vec{v}_0$ is the velocity at the surface cf. [3]. $\mathcal{D}$ is the computational domain and $\mathcal{B}$ the corresponding boundary. The boundary integral accounts for the vorticity not included in $\mathcal{D}$. The particle approximation of (9) is

$$\begin{aligned}\vec{v}(\vec{x}_p) \approx &-\frac{1}{2\pi} \sum_{i=1}^{n_p} \frac{\Gamma_i \vec{e}_z \times \Delta\vec{x}_{i,p}}{|\Delta\vec{x}_{i,p}|^2} \\ &+ \frac{1}{2\pi} \sum_{j=1}^{n_b} \oint_{\mathcal{B}_j} \frac{(\vec{v}_0 \cdot \vec{n}_0)\Delta\vec{x}_{0,p} - (\gamma_0 \vec{e}_z + \vec{v}_0 \times \vec{n}_0) \times \Delta\vec{x}_{0,p}}{|\Delta\vec{x}_{0,p}|^2} \, \mathrm{d}\mathcal{B}_0,\end{aligned} \tag{10}$$

where $\Delta\vec{x}_{0,p} = (\vec{x}_0 - \vec{x}_p)$, n_b is the number of bodies, and n_p is the number of free particles The singular particle-particle interaction in (10) is regularised by

applying a Gaussian core function. The bodies are approximated by polygons and the surface vortex sheet and surface velocity are given a linear variation when evaluating (10).

2.3.3 Vorticity boundary condition

The vorticity boundary condition is found evaluations the normal component of equation (10) at the boundary $\mathcal{B}$ cf. [4] and [5], thus

$$\int_{\mathcal{B}} \frac{\gamma_0 \vec{e}_z \times \Delta\vec{x}_{0,\mathcal{B}}}{|\Delta\vec{x}_{0,\mathcal{B}}|^2} \,\mathrm{d}\mathcal{B}_0 \cdot \vec{n}_{\mathcal{B}} = \vec{\mathcal{J}}(\vec{x}_{\mathcal{B}}) \cdot \vec{n}_{\mathcal{B}} + 2\pi \left[\vec{V}(t) - \vec{v}(\vec{x}_{\mathcal{B}})\right] \cdot \vec{n}_{\mathcal{B}}, \quad (11)$$

where $\vec{\mathcal{J}}$ is the induced velocity from the existing vorticity. The solution of (11) is unique up to constant i.e., an infinite number of solutions exist cf. [3]. The solution is made unique by requiring that time rate of change of the zero-th order vorticity moment

$$\Omega_0 = \iint_{\mathcal{D}} \omega \,\mathrm{d}\mathcal{D}. \quad (12)$$

is conserved ($d\Omega_0/dt = 0$). The discrete approximation of (12) is

$$\Omega_0 \approx \int_{\mathcal{B}} \gamma \,\mathrm{d}\mathcal{B} + \iint_{\mathcal{F}} \omega \,\mathrm{d}\mathcal{F} + \iint_{\mathcal{S}} \omega \,\mathrm{d}\mathcal{S}, \quad (13)$$

where $\mathcal{F}$ denotes the fluid, and $\mathcal{S}$ is the solid body domain. Thus for each j-th body the time rate of change of (12) is conserved

$$\sum_{i=1}^{m_j} \frac{\gamma_{ij}^k - \gamma_{ij}^{a,k-1}}{\Delta t} \Delta s_{ij} + 2A_j \frac{\dot{\alpha}_j^k - \dot{\alpha}_j^{k-1}}{\Delta t} = 0, \quad (14)$$

where m_j is the number of boundary elements on the j-th body, Δs_{ij} is the length of the boundary element, and $\dot{\alpha}_j$ is the angular velocity of the body. $\gamma_{ij}^{a,k-1}$ is the particle strength removed during the previous time from particles entering the body. In (14) it is assumed, that the initial value of Ω_0 is zero.

It can be shown, that the satisfaction of (14) secures a singled valued pressure distribution cf. [6].

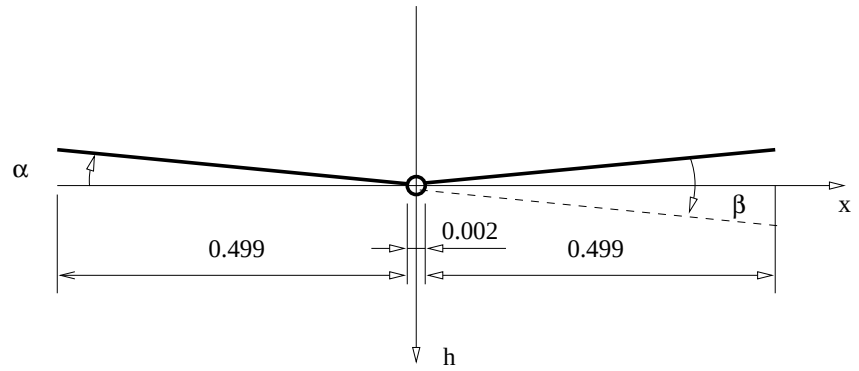

Fig. 2. Sketch of flat plate with half-chord trailing edge flap.

To avoid accumulation of truncation errors, also the global rate of change of the zero-th order vorticity moment is conserved, i.e.,

$$\sum_{j=1}^{n_b}\left(\sum_{i=1}^{m_j}\frac{\gamma_{ij}^{k}-\gamma_{ij}^{a,k-1}}{\Delta t}\Delta s_{ij}+2A_j\frac{\dot{\alpha}_j^{k}-\dot{\alpha}_j^{k-1}}{\Delta t}\right)+\sum_{i=1}^{n_p}\Gamma_i=0. \tag{15}$$

Equations (11), (14), and (15) are solved in the least squares sense.

3 Results

The flow past a flat plate with a half-chord trailing edge flap is simulated for a reduced velocity of $v_r = \pi v/\omega b = 10$ and a Reynolds number based on the chord length of 10^4. The plate has a finite thickness, $w = 0.0025$ and a gap between the main plate and the flap to allow the rotation cf. Fig. 2. The main plate undergoes a pitch motion with an out-of-phase flap motion, thus

$$\alpha(t) = A_\alpha \sin(\omega t), \tag{16}$$
$$\beta(t) = -2\alpha(t), \tag{17}$$

where $A_\alpha = 2^\circ$ is the amplitude of the motion.

Figs. 3 shows the predicted time history of the total lift (L) and moment (Ma), and the moment on the flap alone (Mb). It is clear, that the total moment primarily stems from the loads on the flap. The extracted aerodynamic derivatives are shown in Tables 1 and 2. The corresponding modelled total lift and moment and flap moment are compared with the Theodorsen values in Fig. 4. In general excellent agreement is observed considering the roll-up of the wake and blowing of the boundary layer through the gap — phenonema not included in the inviscid theory cf. [1]. Notice, that the lift force and angle of attack are out of phase, indicating a stable configuration.

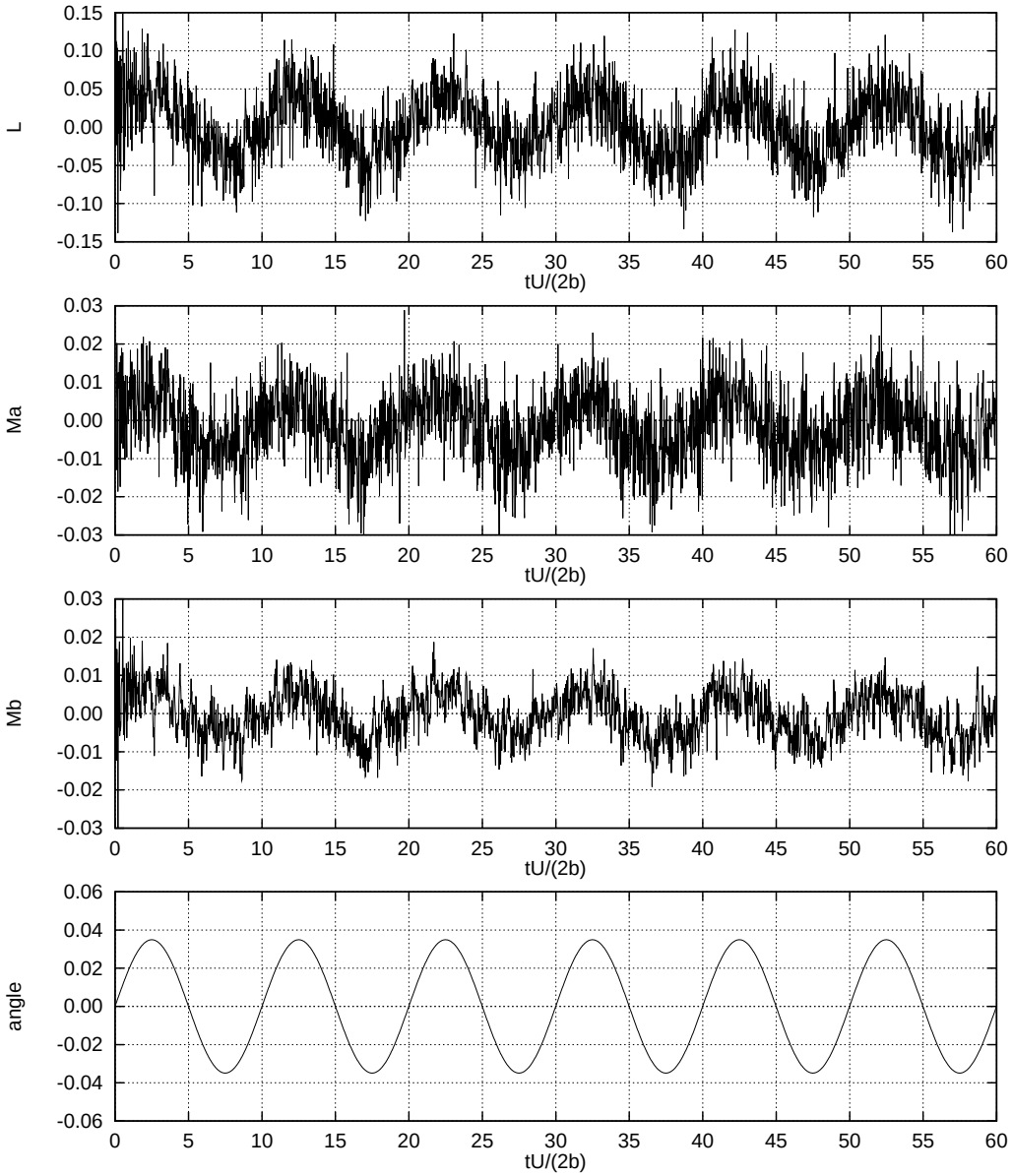

Fig. 3. Time history of the predicted total lift (L) and moment (Ma), and the moment on the flap (Mb) for the flow past a flat plate undergoing pitch motion with out-of-phase flap motion.

	H_2^*	H_3^*
L	1.527	46.53

Table 1
Predicted aerodynamic derivatives for the flat plate.

Fig. 5 shows the instantaneous position of the particles close to the plate at $tU/2b = 57.5$. Particles in the wake are merged to reduce the computational work.

	A_2^*	A_3^*
M_α	5.786	15.30
M_β	2.930	13.40

Table 2
Predicted aerodynamic derivatives for the flat plate and for the trailing edge flap.

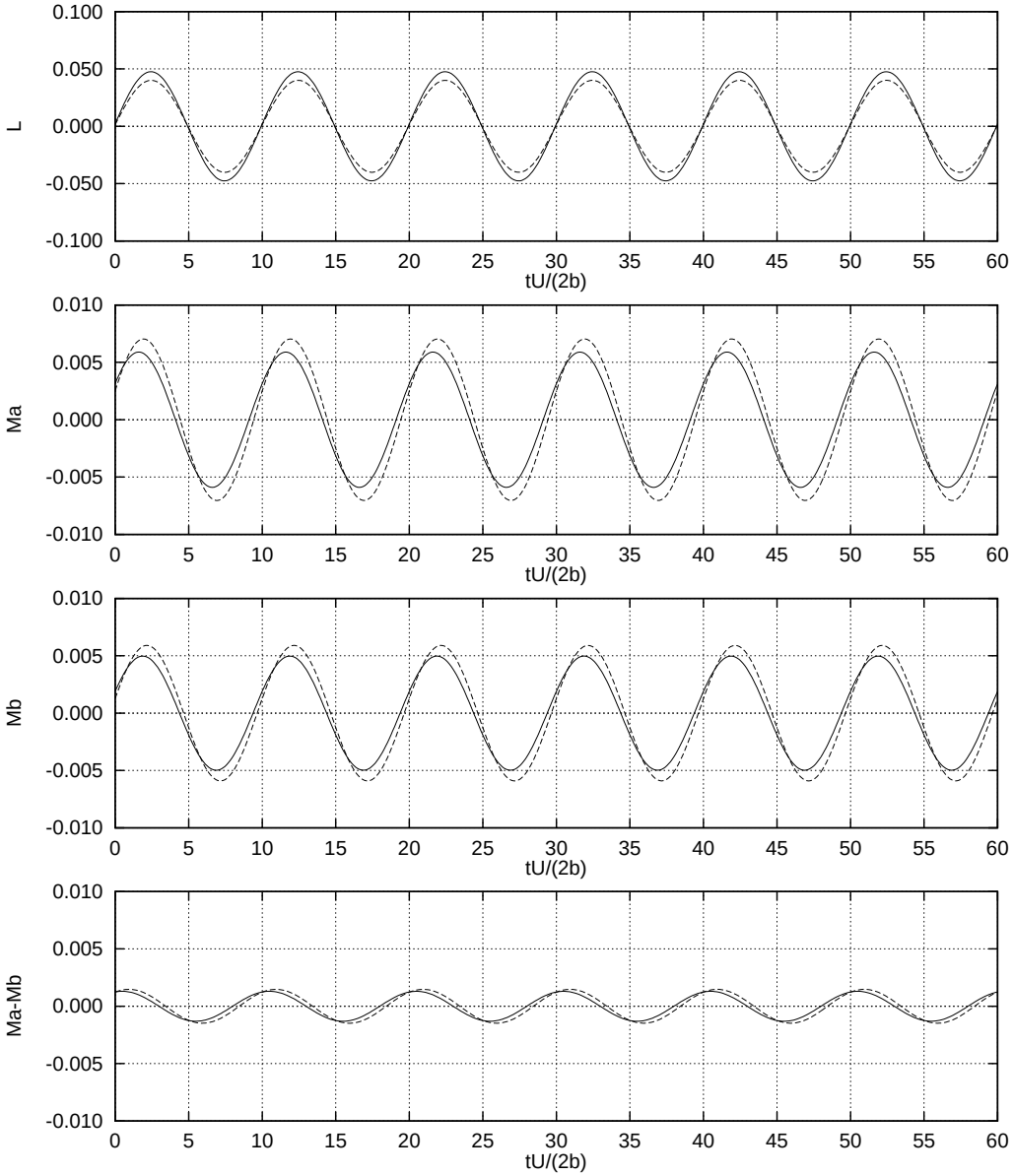

Fig. 4. Time history of the fitted total lift (L) and moment (Ma), and the moment on the front plate (Ma-Mb) and the flap (Mb) for the flow past a flat plate undergoing pitch motion with out-of-phase flap motion. —, theory [1]; – – –, present results.

Fig. 5. Instantaneous position of the particles at tU/2b = 57.5 at maximum angle of attack. The total number of particles is 9694. Particles in the wake are merged to reduce the computation work (not shown).

4 Conclusion

In the present study, the flow past a flat plate with a half-chord flap is simulated using a mesh-free particle method.

The conservation of the time rate of change of the zero-th order vorticity moment is used to obtain a unique solution. Moreover, the conservation of the zero-th order vorticity moment guarantees a singled value pressure distribution for the individual solid bodies.

The flow past the flat plate undergoing a harmonic pitch motion with an out-of-phase flap motion is used as a generic flow past multiple oscillating bodies and as a test of the concept of active flutter control.

The predicted loads are in excellent agreement with the theoretical inviscid lift as given by Theodorsen. Also, the lift force is reversed as compared with the in-phase flap motion increasing the stability of the structure.

A Trigonometric constants

The constants in equations (1) – (3) are cf. [1]

$$
\begin{aligned}
T_1 &= -\frac{1}{3}\sqrt{1-c^2}(2+c^2) + c\cos^{-1} c, \\
T_2 &= c(1-c^2) - \sqrt{1-c^2}(1+c^2)\cos^{-1}(c) + c(\cos^{-1}(c))^2, \\
T_3 &= -\left(\frac{1}{8}+c^2\right)(\cos^{-1} c)^2 + \frac{1}{4}c\sqrt{1-c^2}\cos^{-1} c(7+2c^2) - \frac{1}{8}(1-c^2)(5c^2+4), \\
T_4 &= -\cos^{-1} c + c\sqrt{1-c^2}, \\
T_5 &= -(1-c^2) - (\cos^{-1} c)^2 + 2c\sqrt{1-c^2}\cos^{-1} c, \\
T_7 &= -\left(\frac{1}{8}+c^2\right)\cos^{-1} c + \frac{1}{8}c\sqrt{1-c^2}(7+2c^2),
\end{aligned}
$$

$$
\begin{aligned}
T_8 &= -\frac{1}{3}\sqrt{1-c^2}(2c^2+1) + c\cos^{-1} c, \\
T_9 &= \frac{1}{2}\left[\frac{1}{3}\left(1-c^2\right)^{\frac{3}{2}} + aT_4\right], \\
T_{10} &= \sqrt{1-c^2} + \cos^{-1} c, \\
T_{11} &= (1-2c)\cos^{-1} c + \sqrt{1-c^2}(2-c), \\
T_{12} &= \sqrt{1-c^2}(2+c) - \cos^{-1} c(2c+1), \\
T_{13} &= \frac{1}{2}\left[-T_7 - (c-a)T_1\right].
\end{aligned}
$$

References

[1] Theodore Theodorsen. General theory of aerodynamic instability and the mechanism of flutter. TR 496, NACA, 1935.

[2] Alexandre Joel Chorin. Numerical study of slightly viscous flow. *J. Fluid Mech.*, 57:785–796, 1973. Part 4.

[3] J. C. Wu. Numerical boundary conditions for viscous flow problems. *AIAA J.*, 14(8):1042–1049, 1976.

[4] J. C. Wu and U. Gulcat. Separate treatment of attached and detached flow regions in general viscous flows. *AIAA J.*, 19(1):20–27, 1981.

[5] Jens Honoré Walther. *Discrete Vortex Method for Two-dimensional Flow past Bodies of Arbitrary Shape Undergoing Prescribed Rotary and Translational Motion.* PhD thesis, Department of Fluid Mechanics. Technical University of Denmark, September 1994. Unpublished.

[6] Jens Honoré Walther and Allan Larsen. Discrete vortex method for application to bluff body aerodynamics. *J. Wind Engng. and Industrial Aerodynamics*, 67–68:183–193, 1997.